

Indirect monitoring of mixed conduction in $\text{La}_2\text{NiO}_{4+\delta}$ -based systems using impedance spectroscopy

Yong Hoon Kim^a, Seung Muk Bae^a, Chan-Rok Park^a, Sang-Yun Jeon^b, Moon-Bong Choi^b, Sun-Ju Song^b, Young-Sung Yoo^c and Jin-Ha Hwang^{a,*}

^aDepartment of Materials Science and Engineering, Hongik University, 72-1 Sangsu-dong, Mapo-gu, Seoul 121-791, Korea

^bDepartment of Materials Science and Engineering, Chonnam National University, 300 Yongbong-ro, Buk-gu, Gwangju 500-757, Korea

^cGreen Growth Technology Laboratory, Korea Electric Power Research Institute, 65 Munji-Ro, Yuseong-Gu, Daejeon 305-760, Korea

The Electrochemical activities of updoped ($\text{La}_2\text{NiO}_{4+\delta}$) and Ba-doped lanthanum nicklate ($\text{La}_{1.85}\text{Ba}_{0.15}\text{NiO}_{4+\delta}$) materials were estimated using impedance spectroscopy and digital image processing. Mixed conduction was evaluated with an ionic-conducting, Gd_2O_3 -doped CeO_2 probe. Geometric constriction between the ionic probe and mixed-conducting materials allowed for the relative contribution of ionic conduction with regard to electronic conductivity in terms of polarization losses originating from the interface between the oxygen conductor and the mixed-conduction materials. The electrochemical loss in doped $\text{La}_{1.85}\text{Ba}_{0.15}\text{NiO}_{4+\delta}$ was significantly lower than that measured in updoped $\text{La}_2\text{NiO}_{4+\delta}$. Therefore, Ba-doped lanthanum nicklate appears to provide better ionic conduction compared to the updoped material.

Key words: Mixed conduction, Impedance spectroscopy, Electrochemical losses, $\text{La}_2\text{NiO}_{4+\delta}$.

Introduction

Lanthanum nicklate ($\text{La}_2\text{NiO}_{4+\delta}$)-based materials have been receiving academic and industrial recognition in the form of highly efficient electrochemical systems, including solid oxide fuel cells and ceramic membranes for oxygen separation and partial oxidation of hydrocarbons. [1-3]. The unique features of these materials are due to superior oxygen ion conduction in oxide-based crystal structures [4-9]. It has been proposed that the defect chemistry of $\text{La}_2\text{NiO}_{4+\delta}$ is based on the peculiar structure of the alternatively stacked rock salt-type La-O and Perovskite-type LaNiO_3 . The ionic defects in Perovskite-type LaNiO_3 are extremely small due to difficulty in the formation of oxygen vacancies in the stoichiometric ABO_3 structure. The atomic structure of $\text{La}_2\text{NiO}_{4+\delta}$ allows the introduction of negatively charged oxygen interstitials at the center of the La tetrahedron and facile conduction along the *ab* crystal planes [7, 9]. The layered structure of La-O and LaNiO_3 accommodates a high level of oxygen-based imperfections, including oxygen interstitials. High oxygen hyperstoichiometric and undoped $\text{La}_2\text{NiO}_{4+\delta}$ systems have been reported to contain oxygen interstitials and electronic holes as primary defects [4].

Mixed conduction phenomena have been measured either via electrochemical titration or relaxation measurements

subjected to different electrochemical activities. The work presented here proposes a facile characterization approach toward a fast and relative comparison among mixed conduction materials. We investigated the potential of controlling mixed conduction through doping in La_2NiO_4 -based materials. The model system chosen was composed of undoped La_2NiO_4 and doped $\text{La}_{1.85}\text{Ba}_{0.15}\text{NiO}_4$. The mixed conduction features were analyzed using impedance spectroscopy in combination with microstructural features. In particular, geometric constriction was employed to evaluate the mixed conduction of La_2NiO_4 -based materials. The implications of impedance spectroscopy toward screening and optimizing mixed conduction features and the electrochemical potential of La_2NiO_4 -based materials for ceramic membranes and solid oxide fuel cells are discussed.

Experimental Procedure

Undoped $\text{La}_2\text{NiO}_{4+\delta}$ and doped $\text{La}_{1.85}\text{Ba}_{0.15}\text{NiO}_{4+\delta}$ powders were synthesized from lanthanum acetate hydrate ($\text{C}_6\text{H}_9\text{LaO}_6 \cdot \text{H}_2\text{O}$, 99.9%, Aldrich, USA), nickel acetate tetrahydrate ($(\text{C}_2\text{H}_3\text{O}_2)_2\text{Ni} \cdot 4\text{H}_2\text{O}$, 99.9%, Aldrich, USA) and acetate ($(\text{CH}_3\text{COO})_2\text{Ba}$, 99%, Aldrich, USA) using a coprecipitation method. Calculated amounts of each constituent material were dissolved in distilled water and mixed homogeneously. Subsequently, a small amount of ammonium hydroxide was added to adjust the pH to 10. The controlled solution was dried under stirring conditions and calcined at 1173 K for 10 h under ambient conditions. Crystalline phases of the obtained powders were charac-

*Corresponding author:

Tel : +82-2-320-3069
Fax: +82-2-333-0127
E-mail: jhwang@hongik.ac.kr

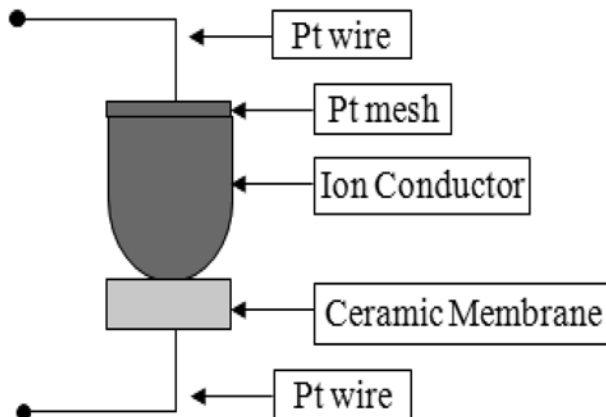


Fig. 1. The schematic diagram of an electrochemical system involving geometric constriction in two-point impedance spectroscopy.

terized using X-ray diffraction (XRD; D/MAX Ultima III, Rigaku, Japan) equipped with a Cu target. The calcined powder was pressed into discs and then placed into the measuring apparatus. The detailed electrode configuration is shown in Fig. 1. The impedance spectra were measured using a Solartron 1260 frequency response analyzer (FRA). After installation into the apparatus, the specimens were annealed at 900 °C for 5 h to guarantee intimate contact between the electrolyte and La₂NiO₄-based materials. The impedance spectra were measured in air at temperatures between 600 and 800 °C. The obtained impedance information was analyzed using an equivalent circuit model.

Results and Discussion

Electrochemical characterization

To investigate the electrochemical performances of the La₂NiO₄-based materials, the electrode configuration involved a two-point impedance configuration, as shown in Fig. 1. In particular, geometric constriction was employed to amplify the bulk and interfacial responses originating from the micro-contacted region with the Gd₂O₃-doped CeO₂ (GDC) used as the ionic conducting probe. Direct contact between the GDC hemispherical portion and the La₂NiO₄-based material produced a significant geometrical constriction in the movement of oxygen ions, leading to higher resistance in the GDC bulk materials and at the electrode/electrolyte interface.

Based on the electrode configuration in Fig. 1, the electrochemical impedance was acquired as a function of temperature between 600 °C and 800 °C in undoped La₂NiO_{4+δ} and doped La_{1.85}Ba_{0.15}NiO_{4+δ}. The high frequency response was attributed to the bulk portion including the ohmic contribution of lead wires, La₂NiO₄-materials, and electrolytes, i.e., GDC. The frequency response of the bulk portion can be estimated mainly due to the geometric constriction between the GDC and La₂NiO₄-based materials. The spreading resistance contribution overwhelmed the high-frequency component due to the lead wires and the smaller bulk electrolyte resistance, which was not associated

with the above spreading resistance. The effective bulk contribution originated from the ionic flow adjacent to the contact point between the electrolyte and the electrode.

The low impedance contribution was ascribed to interfacial polarization between the ionic electrolyte and electrode. The component was largely dependent on charge transfer involving electrons and ions. In the setup described in Fig. 1, the apparent low-frequency data was attributed to the geometrically restricted interfacial response between the GDC electrolyte and the La₂NiO₄ materials. Accordingly, the impedance spectra in Fig. 2 reflect the bulk and interfacial components associated with the geometric constriction. Based on the impedance features of Fig. 2, an equivalent circuit was proposed, as shown in Fig. 3. The R₀ component models the contribution of the bulk GDC electrolytes in the high-frequency region. The latter R₁CPE₁ and R₂CPE₂ components were used to describe the electrode responses between the electrolyte and the La₂NiO₄ materials with the resolved resistive components summarized in Table 1 and Fig. 4. The ratio of the interfacial to the bulk component (R_t/R₀) indicates the relative magnitude of electrochemical polarization loss. Usually, lower electrochemical polarization is achievable in higher mixed conduction systems; therefore, the lower is the

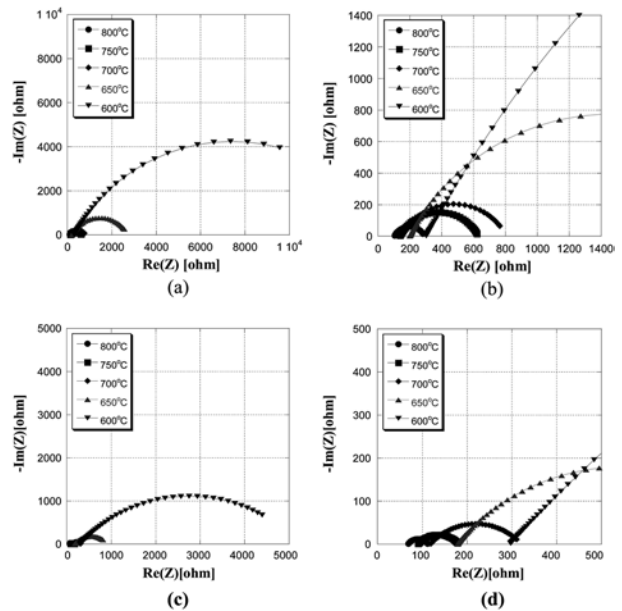


Fig. 2. Impedance spectra obtained from undoped La₂NiO_{4+δ} (a, b) and doped La_{1.85}Ba_{0.15}NiO_{4+δ} (c, d) as a function of temperature between 600 and 800 °C.

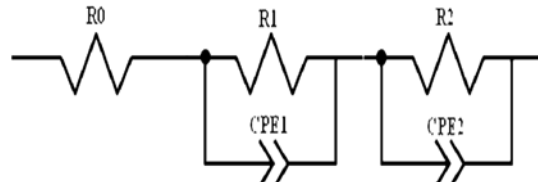
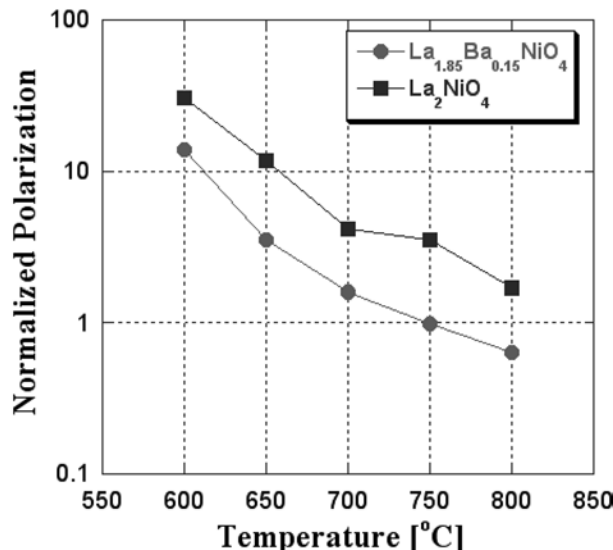


Fig. 3. An equivalent circuit model applied to an electrochemical system involving geometric restriction in two-point impedance spectroscopy.

Table 1. Summary on the analyzed parameters using impedance spectra and the corresponding equivalent circuit [unit: ohm]

$\text{La}_{1.85}\text{Ba}_{0.15}\text{NiO}_4$	R0	Rt	Rt/R0	La_2NiO_4	R0	Rt	Rt/R0
800 °C	68.587	43.633	0.63617	800°C	104.97	177.07	1.686863
750 °C	90.553	88.597	0.9784	750°C	138.04	483.92	3.505651
700 °C	119.11	191.1	1.6044	700°C	149.14	614.93	4.123173
650 °C	178.92	631.95	3.53203	650°C	199.34	2354.56	11.81178
600 °C	296.72	4098.88	13.814	600°C	302.46	9253.54	30.59426

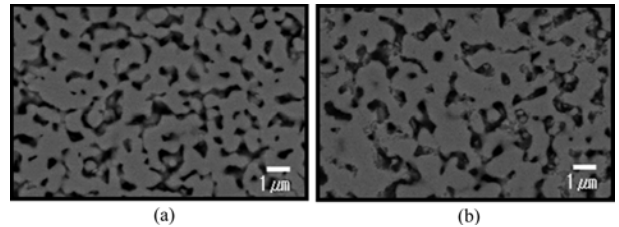
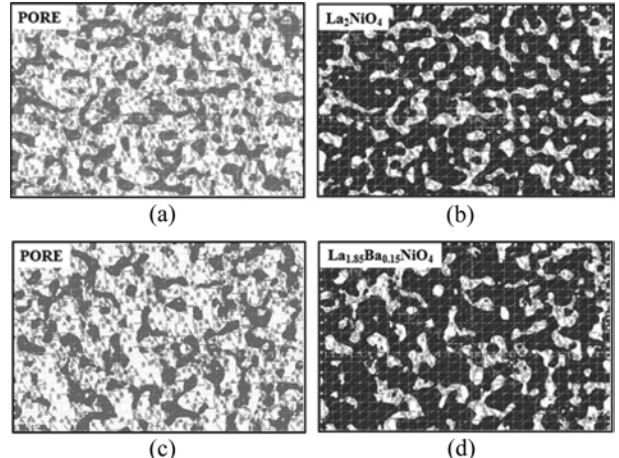
**Fig. 4.** Normalized electrochemical polarization between La_2NiO_4 -based materials and an ionic conductor (Gd_2O_3 -doped CeO_2).

Rt/R0, the weaker is the electrochemical polarization or, equivalently, the higher is the mixed conduction.

Based on the summarized results in Table 1, the electrochemical polarization decreased with increasing temperature. The doped $\text{La}_{1.85}\text{Ba}_{0.15}\text{NiO}_4$ exhibited weaker electrochemical polarization. The lowest parameter (0.636) was found in $\text{La}_{1.85}\text{Ba}_{0.15}\text{NiO}_4$ at 800 °C, and the highest polarization loss (30.594) was found in La_2NiO_4 at 600 °C. The current measurements provide valuable information in that there is a significant increase in electrochemical polarization with decreasing temperature and higher mixed conduction in doped $\text{La}_{1.85}\text{Ba}_{0.15}\text{NiO}_4$. Ba-doping into La-sites incorporated oxygen vacancies into the perovskite LaNiO_3 layer structure in order to meet the charge neutrality conduction involving the alivalent doping of Ba into La-sites. The ionic contribution is enhanced, compared to the original electronic conduction of La_2NiO_4 . The enhanced ionic contribution allowed a decrease in the electrochemical polarization losses. Further characterization will be focused on quantifying the ionic conductivity with regard to electronic conductivity.

Microstructural characterization

To corroborate the above electrochemical measurements, the above undoped $\text{La}_2\text{NiO}_{4+\delta}$ and doped $\text{La}_{1.85}\text{Ba}_{0.15}\text{NiO}_{4+\delta}$ were analyzed in terms of their microstructural aspects,

**Fig. 5.** Electron microscopic images: (a) undoped $\text{La}_2\text{NiO}_{4+\delta}$ (a, b) and (b) doped $\text{La}_{1.85}\text{Ba}_{0.15}\text{NiO}_{4+\delta}$.**Fig. 6.** Examples of quantification based on microstructural images: (a) and (b) undoped $\text{La}_2\text{NiO}_{4+\delta}$ and (c) and (d) doped $\text{La}_{1.85}\text{Ba}_{0.15}\text{NiO}_{4+\delta}$.

as shown in Fig. 5. Stereologic analysis methods [10-14] were employed to evaluate the microstructural images of $\text{La}_2\text{NiO}_{4+\delta}$ and $\text{La}_{1.85}\text{Ba}_{0.15}\text{NiO}_{4+\delta}$. The exemplary lines (horizontal, vertical, and diagonal lines) were applied to the above high-contrast electron image (Fig. 6). The resultant microstructural information is summarized in Table 2 in terms of the line intercepts, area fraction, and interconnectivity (inverse of tortuosity). Assuming that the microstructural images of the La_2NiO_4 -based materials are isotropic, the volume fraction (area fraction) was estimated to be approximately the same at 30% in the porous component and 70% in the solid components. The higher volume fraction in the solid components led to a higher interconnectivity of approximately 83%. The reasonable amount of pores enhanced the appropriate interface reactions involving oxygen gas, oxygen ions, and electrons. The current microstructural similarity simplifies the electrochemical interpretation at the interface between the ionic and mixed-conducting materials. The electrical performance

Table 2. Analyzed microstructural parameters in (a) undoped $\text{La}_2\text{NiO}_{4+\delta}$ (a, b) and (b) doped $\text{La}_{1.85}\text{Ba}_{0.15}\text{NiO}_{4+\delta}$

	Phase	Mean Line Intercept	Area Fraction	Interconnectivity
La_2NiO_4	Pore	0.792	0.297	0.1637
	Solid	0.365	0.703	0.8373
$\text{La}_{1.85}\text{Ba}_{0.15}\text{NiO}_4$	Pore	0.830	0.292	0.1634
	Solid	0.389	0.708	0.8366

can be attributed to the corresponding defect chemistries. The beneficial features of $\text{La}_{1.85}\text{Ba}_{0.15}\text{NiO}_{4+\delta}$ seem to originate from the enhanced ionic contribution compared to the electronic defects.

Conclusions

Undoped $\text{La}_2\text{NiO}_{4+\delta}$ and doped $\text{La}_{1.85}\text{Ba}_{0.15}\text{NiO}_{4+\delta}$ were estimated in terms of mixed conduction. The mixed conduction features can be characterized by monitoring the electrochemical polarization between La_2NiO_4 -based materials and an ionic conductor. The lower polarization indicates that doping of Ba into the La-site increased the formation of oxygen vacancies in the perovskite layer, enhancing the ionic conduction in La_2NiO_4 -based systems. The enhanced ionic contribution can be exploited to synthesize hydrogen gas through a ceramic membrane systems based on La_2NiO_4 -based materials.

Acknowledgement

This research was supported by Basic Science Research Program through the National Research Foundation of

Korea (NRF) funded by the Ministry of Education, Science and Technology(2009-0090172).

References

1. F. Mauvy, C. Lalanne, J.M. Bassat, J.C. Grenier, H. Zhao and P. Dordor, Ph. Stevens, *J. Eur. Ceram. Soc.*, 25 (2005) 2669-2672.
2. J.B. Smith and T. Norby, *J. Electrochem. Soc.*, 153 (2006) A233-238.
3. V.V. Kharton, A.A. Yaremchenko, A.A. Valente, V.A. Sobyanin, V.D. Belyaev, GL. Semin, S.A. Veniaminov, E.V. Tsipis, A.L. Shaula, J.R. Frade and J. Rocha, *Solid State Ionics* 176 (2005) 781-791.
4. M.V. Patrakeev, E.N. Naumovich, V.V. Kharton, A.A. Yaremchenko, E.V. Tsipis, P. Nunez and J.R. Frade, *Solid State Ionics*, 176 (2005) 179-188.
5. J.A. Kilner and C.K.M. Shaw, *Solid State Ionics*, 154-155 (2002) 523-527.
6. J.D. Jorgensen, B. Dabrowski, S. Pei, D.R. Richards and D.G. Hinks, *Phy. Rev. B*, 40 (1989) 2187-2199.
7. J.M. Bassat, P. Odier, A. Villesuzanne, C. Marin, M. Pouchard, *Solid State Ionics*, 167 (2004) 341-347.
8. E.N. Naumovich, M.V. Patrakeev, V.V. Kharton, A.A. Yaremchenko, D.I. Logvinovich and F.M.B. Marques, *Solid State Sciences* 7 (2005) 1353-1362.
9. L. Minervini, R.W. Grimes, John A. Kilner and K.E. Sickafus, *J. Mater. Chem.*, 10 (2000) 2349-2354.
10. K.-R. Lee, S.H. Choi, J. Kim, H.-W. Lee and J.-H Lee, *Journal of Power Sources*, 140 (2005) 226-234.
11. D. Simwonis, F. Tietz and H. Tagawa, *Solid State Ionics* 132 (2000) 241-251
12. K.B. Alexander, P.F. Becher, S.B. Waters and A. Bleier, *Journal J. Am. Ceram. Soc.* 77[4] (1994) 939-946.
13. C.S. Smith and L. Guttman, *Trans. Metall. Soc. AIME* 197 (1953) 81-87.
14. J.W. Cahn and J.E. Hilliard, *Trans. Metall. Soc. AIME* (1959) 759-761.